

Explosion-Protecting Chambers for Investigating Hydrodynamic Processes and Explosive Technologies (Review)

M. A. Syrunin and V. A. Ogorodnikov

Russian Federal Nuclear Center, All-Russian Scientific Research Institute of Experimental Physics,
ul. Mira 37, Sarov, Nizhni Novgorod oblast, 607188 Russia

e-mail: postmaster@ifv.vniief.ru

Received February 10, 2014; in final form, July 28, 2014

Abstract—Within the framework of the scientific trend that was developed at the Russian Federal Nuclear Center, All-Russian Scientific Research Institute of Experimental Physics, explosion-protecting chambers (EPCs) of different types with working volumes ranging from $\sim 10^{-3}$ to ~ 10 m³ were developed and constructed. They are able to hermetically localize explosion products from explosive charges of units of grams to tens of kilograms (in the trinitrotoluene equivalent (TNTE)). Scientific and engineering approaches to designing the EPC structures, which are based on experimental methods and numerical simulation, are presented. Examples of developed chambers that are used in studies of a number of hydrodynamic processes are given.

DOI: 10.1134/S0020441215020128

When performing physical investigations of hydrodynamic processes and developing a number of intense technologies, explosives are widely used as loading devices that produce high pressures and temperatures. A shock wave, gaseous explosion products, and high-velocity fragments of inert elements that are produced upon detonation of explosives propagate at a high velocity and exert an effect on the environment as damaging factors of an explosion. One of the ways to protect the environment against their effect is to localize an explosion in a closed volume of an explosion-protecting chamber or container (EPC). EPCs are intended for investigating the properties of materials at high pressures and temperatures, testing explosives and ammunition, evacuating and exterminating terrorist devices, and safely transporting and storing explosive-containing objects. Chambers are also used in explosive technologies, e.g., in explosion welding, and in some engineering fields where the explosion energy is used. An object that contains explosives is placed in an EPC, and the forming explosion products (gases, fragments, and aerosols) are localized in its volume. In this case, when performing the protective function, an EPC must provide registering of the parameters of dynamic processes in an investigated object using various measuring transducers and, consequently, must have appropriate hermetic inputs (outputs) for transmitting electric signals and proton, neutron, X-ray, or optical radiation beams. It is especially pressing to use EPCs when dealing with danger-

ously explosive objects that contain radioactive or toxic substances.

The general scheme of the EPC design is shown in Fig. 1. The chamber contains the following main elements: hermetic pressure housing 1 with bottoms 2; charging orifice 3 that is closed with lid 4; and a protective structure that consists of case 5, bottoms 6, lid 7, and support 8. Dangerously explosive object 9 should be placed, if possible, at the geometrical center of the EPC in order to provide axially symmetric loading of the structure upon an object explosion. The

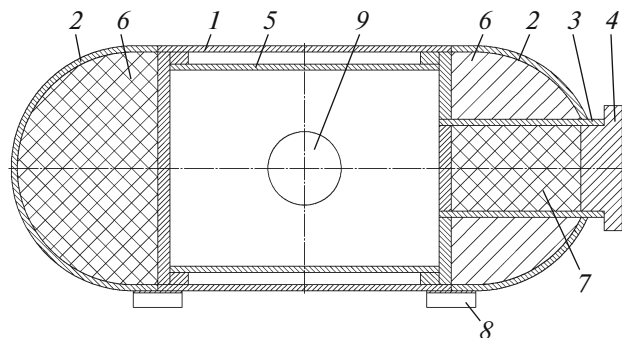


Fig. 1. General scheme of the EPC: (1) load-bearing hermetic housing; (2) bottoms; (3) loading orifice; (4) lid; (5) housing protection; (6) bottom protection; (7) lid protection; (8) supports; and (9) dangerously explosive object (explosive charge).

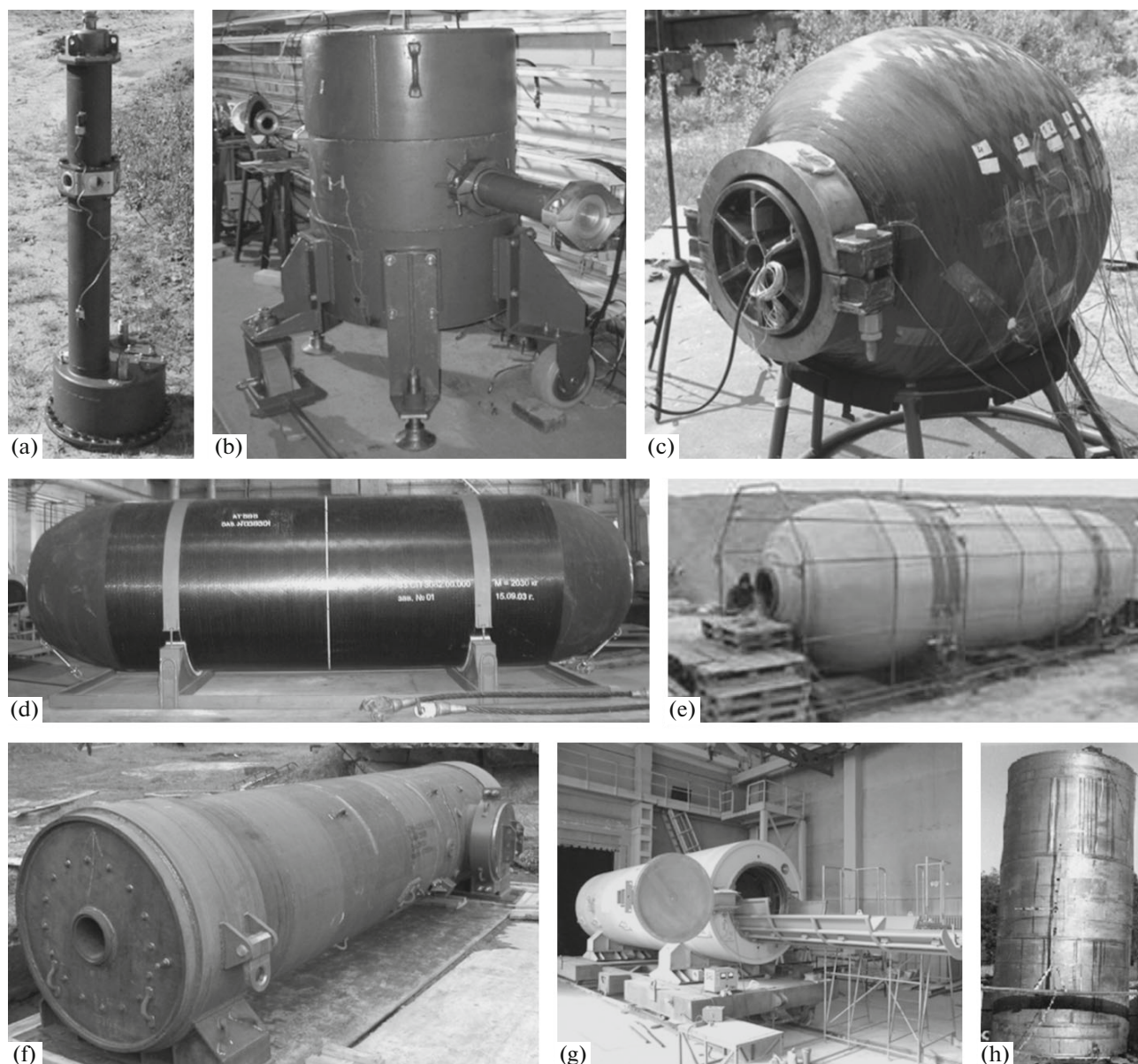


Fig. 2. Explosion-protective chambers of different purposes: (a) compact EPC for optical and X-ray diffraction measurements ($d_{\text{out}} = 0.42$ m, $L = 1.0$, $d_{\text{ch}} = 0.1$ m, $M_c = 70$ kg, $m_{\text{exp}} = 0.015$ TNTE kg) [15]; (b) EPC for radiography ($d_{\text{out}} = 0.82$ m, $L = 1.1$ m, $d_{\text{ch}} = 0.23$ m, $M_c = 980$ kg, $m_{\text{exp}} = 2.5$ TNTE kg) [9, 10, 14]; (c) spherical EPC ($d_{\text{out}} = 0.88$ m, $L = 0.95$ m, $d_{\text{ch}} = 0.22$ m, $M_c = 470$ kg, $m_{\text{exp}} = 5.4$ TNTE kg) [13]; (d) EPC for emergency ammunition ($d_{\text{out}} = 0.99$ m, $L = 3.31$ m, $d_{\text{ch}} = 0.43$ m, $M_c = 2000$ kg, $m_{\text{exp}} = 11.2$ TNTE kg, the mass of the inert ammunition packet is 40 kg) [12]; (e) “Kolba” EPC ($d_{\text{out}} = 2.66$ m, $L = 9.2$ m, $d_{\text{ch}} = 0.55$ m, $M_c = 25$ t, $m_{\text{exp}} = 200$ TNTE kg) [1]; (f) EPC for radiography ($d_{\text{out}} = 1.42$ m, $L = 6.2$ m, $d_{\text{ch}} = 0.65$ m, $M_c = 25$ t, $m_{\text{exp}} = 40$ TNTE kg) [11]; (g) EPC for emergency ammunition ($d_{\text{out}} = 1.79$ m, $L = 6.5$ m, $d_{\text{ch}} = 1.0$ m, $M_c = 25$ t, $m_{\text{exp}} = 60$ TNTE kg) [6]; (h) 12X18H10T steel EPC ($d_{\text{out}} = 2.44$ m, $L = 5.6$ m, $d_{\text{ch}} = 0.5$ m, $M_c = 20$ t, $m_{\text{exp}} = 100$ TNTE kg) [1].

bearing capacity (blast resistance) of the EPC, i.e., the ability to localize the energy release and explosion products of an explosive charge, is provided by the strength and hermeticity of the EPC housing, bottoms, lids, inlets (windows), and other elements. The blast resistance of the EPC is determined by its material, shape, and dimensions; the explosive-charge shape (dimensions) and mass; the location of the detonation-initiation point in the explosive charge; and

the surrounding of the explosive charge (the presence of the housing, metallic inserts, etc.) and its position in the EPC. Depending on their purpose and carrying ability, EPCs have different overall-dimension and weight characteristics.

Some designs of the EPCs with working volumes of 10^{-3} to 10 m³, which can hermetically localize explosion products of charges ranging from several grams to tens of kilograms (in the TNT equivalent (TNTE)),

are shown in Fig. 2 [1–15] (the main EPC parameters have the following notation: L , the EPC length; d_{out} , the outer diameter; d_{ch} , the diameter of the charging orifice; M_c , the EPC mass; and m_{exp} , the maximum mass of the explosive charge (converted into the TNTE), whose explosion is localized in the EPC).

In their purpose, EPCs are subdivided into stationary (which are not displaced during their operation) and transportable and those singly and multiply used for keeping products of fragmentation and fragmentation-less explosions. As to the shape of their closed load-bearing shell, EPCs are subdivided into cylindrical ones with flat and rounded (hemispherical, ellipsoidal, conical) bottoms and spherical chambers. As regards their load-bearing scheme, EPCs are subdivided into single- and double-contour devices (with an inner load-bearing housing that receives the pulse component of the explosion load and an outer load-bearing housing that receives the excess quasi-static pressure of gaseous explosion products).

In the case of a cylindrical shape of the load-bearing housing, EPCs may differ in the method used to protect bottoms against the longitudinal component of the pulse component of an explosion load. The bottom protection systems are either of damping (with flat deformable or massive undeformable diaphragms and dampers of foam plastic, claydite, a stack of a metallic grid, tubes, ribbed elements) or throttle nature (in the form of baffles of disks with one or several holes) [1–3, 5–13].

As regards the applied materials for the main load-bearing element (the housing shell), EPCs are subdivided into single-layer steel and multilayer steel, steel–concrete, steel–composite, and reinforced-concrete chambers [1–15]. When developing the load-bearing housing, one should use structural materials that are characterized by an increased specific strength and energy dissipation under loading, a high thermal and corrosion resistance, and provide a minimally possible sensitivity of the structure to the effect of the scaling factor and defects. Several EPC designs were implemented with load-bearing housings made of alloyed steels, such as 20 steel (Figs. 2a, 2b), 09G2S steel (Fig. 2g), pipe steel of strength class of at least K60 (Fig. 2f), and 12X18H10T stainless steel (Fig. 2h). Titanium and aluminum alloys and composite materials are also the most promising materials [1]. If it is necessary to strengthen the protection of the load-bearing housing against the influence of fragments and jets, an additional (antifragmentation) layer is installed in front of the shell, for which the following elements can be used: steel-grid layers, a set of metal rings, one or several sheet-steel layers, an aluminum alloy, concrete, claydite–concrete, ceramics, sand, etc. [1–15].

The design of each EPC is developed for solving particular typical engineering problems in accordance with the requirements that are more stringent than for

ordinary high-pressure vessels. The basic requirements are as follows: the complete damping of a shock-wave pressure pulse and explosion products; retaining of the structure integrity and a specified degree of hermiticity under the action of pulsed and quasi-static loads, fragments, and other explosion factors; and prevention of a dangerous effect of an explosion on the environment. The obligatory requirements also include the convenience and safety of an EPC, including such types of works as the placement of a dangerously explosive object into an EPC and extraction of this object from it (if necessary); loading, transporting, and unloading of an EPC; performing explosions in it, whose gaseous products produce an excess pressure in the EPC cavity; blowing gases (CO , CO_2 , NO) that contain detrimental, toxic, or radioactive substances in the form of impurities and aerosols out from the EPC; ventilation and purification of the EPC cavity; flaw detection; replacement of elements that exhausted their service life; and some other types of operations.

It should be also noted that the materials that are used in the load-bearing EPC housing and are placed in the most loaded zones, e.g., in the cross section that is positioned at a minimum distance from the explosive-load source, operate at a high-intensity dynamic and nonuniformly distributed load at limiting tolerable strength characteristics. In this case, if an EPC is a singly used device, it cannot be preliminarily tested after manufacturing with an excess gas pressure, which is close to or exceeds the operating pressure, as is done with high-pressure vessels. This is associated with the fact that in such tests, the material of the load-bearing shell will get hazardous damages and plastic deformations, which will not allow the geometry and mechanical properties to be recovered after the load removal. Subsequently, this may cause an EPC failure under the operating load.

The main load-carrying element of the EPC is its load-bearing contour. The material of the load-bearing contour determines the levels of allowable stresses and deformations in the structure upon explosive loading and the character of its reaction and destruction. The shape and dimensions of the load-bearing contour influence both some features of the gas-dynamic processes that occur upon an explosion of an explosive charge and the distribution of shock-wave loads on the closed EPC contour. The aforementioned parameters of the structure determine the value of the total (incident and reflected) pressure pulse acting on the load-bearing contour, i.e., the dynamic and quasi-static loads applied to it. The strength and rigidity of the load-bearing EPC contour depend on the dimensions and location of the charging port (or ports and inlets), and the elements that protect the housing, bottoms, and lids may reduce and redistribute the loads on the EPC elements.

The mass (dimensions) and shape of the explosive charge specify the amplitude and duration of the pressure pulse that acts on the load-bearing EPC housing during an explosion. The inert elements that surround the explosive charge or are positioned inside it are accelerated, deformed, and destructed owing to the explosion energy that is transferred to them; together with the shock wave and gaseous products, they form a loading pressure pulse, which exerts an effect on the EPC shell. Some features of the action of fragments of inert elements, which scatter in the form of a field of fragments with different velocities or a formed directed jet stream of a gaseous medium or a cumulative jet (e.g., upon a point initiation of a spherical explosive charge with a central cavity), may substantially modify the EPC response and result in its local damage. The position of the initiation point in an object influences the explosive-detonation asymmetry, thus leading to deformations of the jet streams and directed fields of fragments, i.e., causing asymmetric loading of the EPC.

The development of the EPC structure must be accompanied by tests of its prototypes for their blast resistance, including trials under increased and destructive explosion loads. For EPCs with sufficiently large dimensions and a high cost, it is desirable to perform such tests on smaller-size models, which are geometrically similar to full-scale prototypes, and, if possible, under other conditions being the same (identical designs, material, production technology, loading technique, environment, etc.) [1]. However, it is known that as the model size decreases, its strength may increase. Consequently, the safety margin that is determined for such a model and transferred to an actual structure will be overestimated and the actual EPC strength margin may be insufficient.

The physical manifestations of the influence of the scale factor on the strength of the EPC structure (the scaling effect) may be diverse, because they are related to the bearing capacity of the structure, the strength characteristics (e.g., the breaking stress σ_{br} or breaking strain ϵ_{br}), the destruction type and character (ductile or brittle, catastrophic), and the destruction location. The scaling effect can be correctly estimated by comparing the response of geometrically similar structures to similar loading. In the case of a geometrical similarity, the relationships $V/L^3 = \text{const}$ and $F/L^2 = \text{const}$ (V is the volume, L is the characteristic size, and F is the cross-sectional area of the structure) are valid, and similar loading is possible only if the “loaded structure—loading machine” systems are similar. The similarity of such systems in static tests is usually not observed because it is difficult to realize; however, it can be successfully realized in explosion tests, if the relationship $V/L^3 = \text{const}$ and $F/L^2 = \text{const}$ is valid (m is the explosive mass, and M is the mass of the loaded structure or its explosion-deformed part). The fulfillment of this condition provides the similarity of

stressed—deformed states (in view of the correction for a difference between the deformation rates) [1].

The manifestation of the scaling effect is accompanied by an abrupt decrease in the bearing capacity of the structure, as its dimensions increase, and a brittle catastrophic character of its destruction.

The results of experimental investigations showed that there exist methods for weakening and even avoiding the influence of the scaling effect [1]. This influence can be weakened, e.g., owing to the use of materials in which there is a combination of the required destruction strength and ductility with a high plasticity, e.g., stainless or alloyed steels [1]. Another method, in which two trends can be distinguished, is a modification of structures. The first method is associated with the influence of the shape of a structure on its sensitivity to the scaling effect. For example, the stressed—deformed states of cylindrical and spherical shells under internal pulsed loading are substantially different: a cylindrical shell is in a state that is close to a uniaxial (circumferential) tension, and a spherical shell is in a biaxial stressed state. As compared to the cylindrical shell, under the same conditions (dimensions, load, etc.), the elastic energy that is stored in a unit volume of the spherical shell is twice as large; therefore, it is more sensitive to the influence of the scaling effect and is fractured more catastrophically [1]. The second method is associated with an increase in the structure size without changes in the characteristic size of load-bearing elements, which take loads on themselves. Thus, the scale factor has a weak or virtually no effect on the strength of shell structures that are formed of fiber composites, rolls of thin steel sheets, and ropes. This is caused by the fact that despite changes in the dimensions of structures, the characteristic sizes of load-bearing elements, e.g., the diameter of fibers in the composite, the diameter of wires in the rope, or the sheet thickness in the roll, remain constant; thus, the fraction of the stored elastic energy that is expended for their destruction remains constant [1, 4–6].

There is a positive experience in developing EPCs in which the role of a load-bearing layer is played by a fiber composite, which is formed by a layer-by-layer-wound specified structure of threads of thin (with a diameter of ~ 0.01 mm) glass fibers, which are impregnated with a polymer binder. In this case, a strong scaling effect is absent, because identical fibers are destructed upon attainment of identical deformations in both the model and the full-scale object, and the stored elastic energy for destruction of an individual fiber is taken from the vicinity of this fiber near a crack. In particular, it was established in [1, 4, 5, 12, 13] that the explosion-loaded geometrically similar cylindrical shells of oriented glass-fiber plastic are fractured at $\xi_{br} = \text{const}$ and $\epsilon_{br} = \text{const}$, thus signifying the absence of a strong scaling effect. The presence of defects on individual fibers, which lead to their rup-

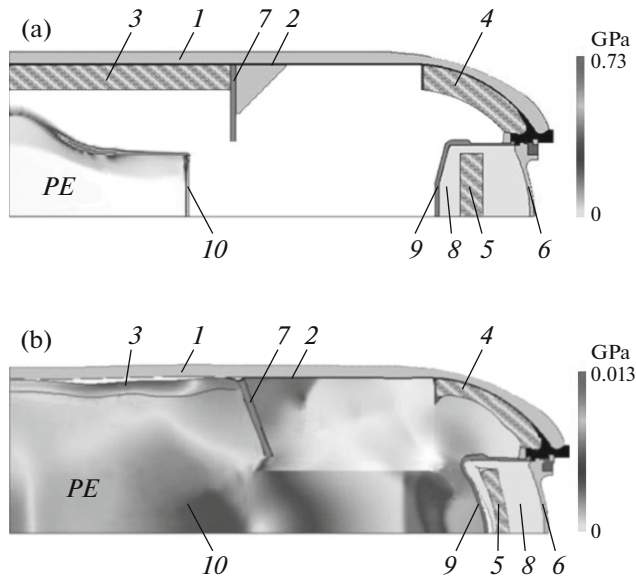


Fig. 3. Calculation scheme of loading with an explosion of an explosive charge with $m_{\text{exp}} = 11.2$ TNTE kg from the geometrical center of a quarter of the cross section of a cylindrical metal–composite EPC with hemispherical bottoms (Fig. 2d) for two moments of time: (a) $t = 137 \mu\text{s}$, (b) $t = 1800 \mu\text{s}$; (1) basalt-plastic shell; (2) steel shell; (3–5) metallic-grid layers; (6) orifice lid; (7) throttle; (8) foam-plastic damper; (9) inner lid; (10) inert case of the explosive charge; and (PE) distribution field of the explosion-product pressure in the EPC cavity cross section [12].

tures in the corresponding cross sections, cannot abruptly reduce the strength of the shell as a whole, because the probability of the coincidence of defects on several thousand fibers that are laid in parallel in a given cross section is negligibly low. The shells that are made of glass-fiber plastic and basalt plastic with epoxy matrices using the winding method are characterized by a high specific strength and a high corrosion resistance, are insensitive to the influence of the scaling factor, and have a low sensitivity to small defects [1, 12]. They are destructed in the elasticity region and have a high energy capacity.

The relatively low thermal stability of the matrix, the low cyclic strength, and the dynamic instability of shells manufactured of the aforementioned composites under pulsed loading [1] are the main drawbacks that impose limitations on the independent application of these materials for the load-bearing EPC housing. However, it was established in [1, 4, 5] that the strengthening of glass-fiber and basalt plastic on the inside with a steel shell allows these drawbacks to be eliminated. The steel layer specifies the shape of the housing shell, blocks the dynamic instability of the composite layer, reduces the thermal loads, and provides the EPC hermeticity. A metal–composite structure absorbs a much higher energy than that absorbed by a steel EPC. For example, this provides the solution

of problems that are related to mass limitations; this is important for the EPC transportability. Such EPCs were successfully used as the main explosion-protecting contour in physical experiments and in explosion-protecting containers for evacuating emergency ammunition and terrorist devices (Figs. 2c–2e) [1, 12–15]. The weight-perfection index (the ratio of the explosive-charge mass, whose explosion is localized within a container, to the mass of this container) of spherical metal–composite EPCs is 1.1–2.5%, which exceeds the index of analogous metal containers by a factor of >2 [1, 3, 4, 13].

Singly used EPCs that are manufactured of steels usually allow slight plastic deformations (1–2%) in the most loaded parts of their structures, because otherwise one fails to obtain acceptable mass–dimensional characteristics for them. Therefore, before each explosion test of such an EPC with a specified loading level, it is necessary to perform a computational and experimental substantiation of its strength and reliability provided that the condition for the operation of the material of the load-bearing housing is surely fulfilled in the region of elastic deformations. If slight plastic deformations are allowed in some zones of the most stressed EPC cross sections, their values cannot reach the experimentally verified levels of obviously “non-destructive” deformations (stresses), which are approximately one order of magnitude lower than the “limiting” (that are close to destructive) values [16].

For metal EPCs that can be used many times, the allowed stresses (deformations) for the load-bearing housing are even lower; this means that at the same loads, their dimensions and mass become larger or the mass of the exploded charges decreases in comparison to singly used structures.

When EPCs are developed, computational and experimental investigation methods are widely used. Specialized software systems have been developed, which are used to calculate the gas-dynamic loads that arise upon an explosion of an explosive charge and to determine the stressed–strained state of the EPC elements during their response to explosion-induced loads [17–20]. The DIADA2D software system for calculating the gas-dynamic loads on structural elements of EPCs is based on the use of S.K. Godunov’s method [17–19]. This method is based on the solution of the problem of a decay of an arbitrary explosion. The calculation of a flow is performed in movable Euler coordinates and allows one to distinguish shock and detonation waves and contact explosions. Examples of the calculation of an explosion of a compact explosive charge with $m_{\text{exp}} = 11.2$ TNTE kg, which is surrounded by a multilayer housing with a mass of 40 kg in a cylindrical metal–composite EPC (Fig. 2d) are presented in Fig. 3, which shows the fields of the explosion-product pressure distribution and the arrangement and shape of both the main structural elements of the EPC and the explosive-charge case at

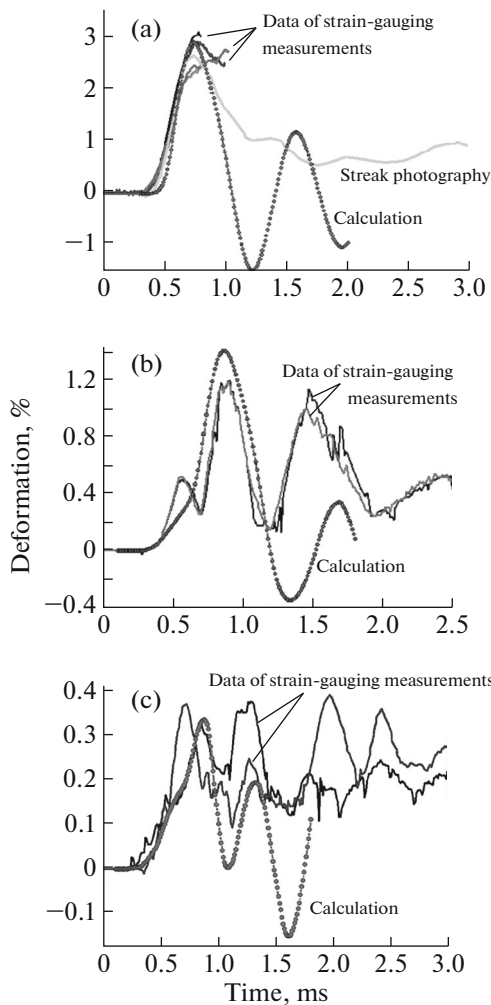


Fig. 4. Comparison of the calculated (dotted lines) and experimental (data from strain-gauging measurements) time dependences of the circular deformation in the cylindrical shell of a metal–composite EPC (see Fig. 2d): (a) in the central cross section where an explosive charge was installed; and (b, c) in the cross sections lying at distances of 400 and 625 mm from the central cross section, respectively. The explosive load is $m_{\text{exp}} = 11.2$ TNTe kg; in the central cross section, after the attainment of the first deformation maximum, the signal from strain gauges at the moment of ~ 1.0 ms disappeared because of their damage [12].

two moments of time for a quarter of the EPC cross section [12].

Calculations of a stressed–strained state of the EPC elements with consideration for a nonlinear behavior of the material and a contact interaction under explosion-induced intense mechanical and thermal loads are conducted using the DRAGON software system [20]. Figure 4 shows the comparison of the experimental results and some calculation results in the form of the time dependences of a “circular” deformation of the cylindrical EPC shell in several cross sections along its generatrix. These depen-

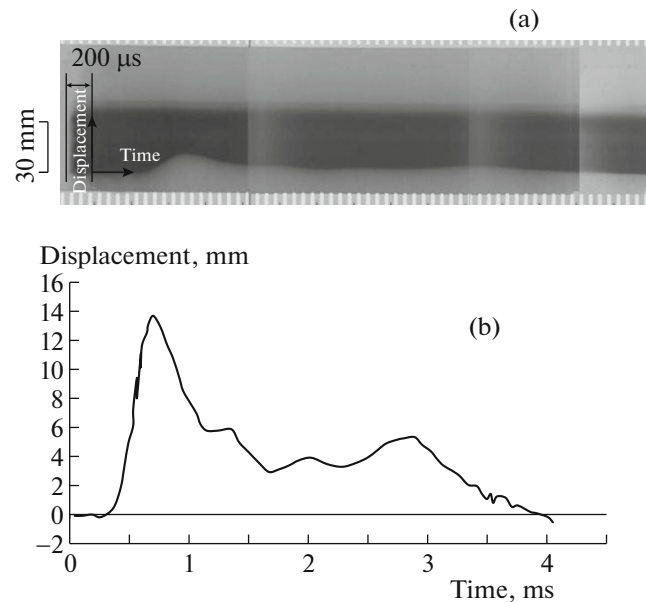


Fig. 5. (a) Streak photograph and (b) results of its processing in the form of the time dependence of the radial displacement, which were obtained in an explosion test of a cylindrical metal–composite EPC, which is shown in Fig. 2d, using an explosive charge with $m_{\text{exp}} = 11.2$ TNTe kg [12, 21].

dences characterize the EPC response to the aforementioned explosive load (Fig. 3) [12].

Experimental investigations of the EPC under explosive loading include the following:

- (i) tests of new designs of EPCs and separate elements;
- (ii) model and full-scale tests of load-bearing structural elements;
- (iii) model tests of the structure as a whole;
- (iv) full-scale tests for confirming the bearing capacity and strength margins;
- (v) service tests of the EPC.

Investigations make it possible to reveal the features of the reactions of the newly developed design, to optimize its structural scheme and separate load-bearing elements, to determine the bearing capacity and strength margins of the EPC, to certify it for one-time or multiple use, to confirm the strength service life of the EPC during its operation, and to obtain data for testing the calculation programs that are used in the numerical simulation, which accompanies all experiments.

To obtain the necessary information on the blast resistance and industrial safety of an EPC during its experimental refinement and operation for determining its strength parameters, which characterize its response to explosive and subsequent quasi-static loadings, well-known and specially developed measurement diagnostic methods [1, 5, 12, 13, 21] are widely used. Displacements and deformations of EPC

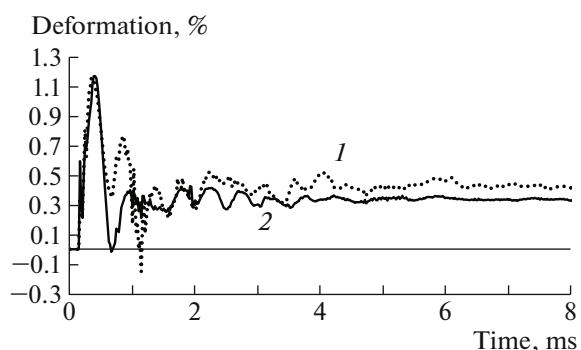


Fig. 6. Time dependences of the circular dynamic deformations, which were obtained in an explosion test of a spherical EPC (shown in Fig. 2c) using an explosive charge with $m_{\text{exp}} = 5.4$ TNTE kg. Strain gauges were placed (1) in the equatorial cross section and (2) at a distance of 200 mm from the equator along the generatrix [13].

elements are recorded as functions of time using such methods as high-speed photochronography (Fig. 5), strain gauging (Fig. 6), electric-contact measurements, and high-speed filming (Fig. 7). High-speed photochronography is performed via the frame or shadow method. An object is placed between a high-power pulsed light source and the objective lens of the high-speed recorder. Figure 5 shows a streak photograph of the time-dependent radial displacement of the EPC outer surface (Fig. 2d) in the most severely

loaded central cross section, which was obtained using the shadow recording method in the “slit” mode. This cross section coincides with the center of the explosive charge with the mass $m_{\text{exp}} = 11.2$ TNTE kg. The results of processing the streak photograph in the form of the “displacement–time” dependence are shown in this figure.

The motion velocities of the EPC-housing surface in specified cross sections are recorded with laser and radio interferometers and a capacitive sensor, and the accelerations (overloads) are registered with piezoelectric accelerometers. The pulse and residual pressures in the EPC and the temperatures in its cavity and at the walls are also measured.

To date, a compact EPC with a bearing capacity of 15 TNTE g [15] and a Kolba transportable container, which withstands an explosion of up to 200 TNTE kg [1] (Figs. 2a, 2e), have been used in the practice of physical investigations at the Russian Federal Nuclear Center–All-Russian Scientific Research Institute of Experimental Physics. EPCs of different modifications with load-bearing housings of steel, steel and concrete, and composite materials and steel were developed for localization of explosions with energies of up to 50 TNTE kg. Some of them are successfully operated. An example of recording the process of ejection (sputtering) of particles from the free surface of a lead sample, which was subjected to shock-wave loading with a maximum amplitude of the loading pressure pulse of ~ 15 GPa, are presented in Fig. 8 [15].

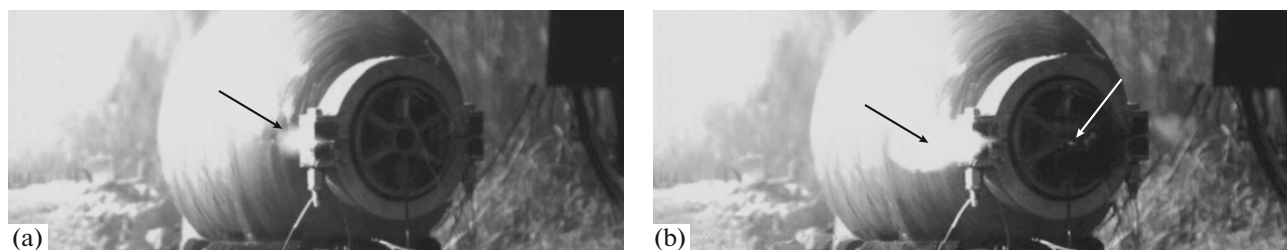


Fig. 7. Frames of high-speed video filming of tests of a spherical EPC (shown in Fig. 2c) for different moments of time (the arrow shows the place from where gases outflow): (a) $t = 1$ ms and (b) $t = 2$ ms [21].

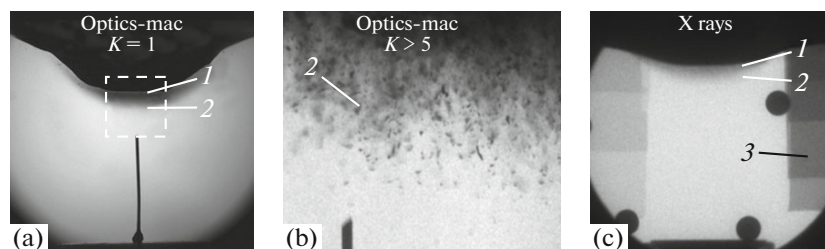


Fig. 8. Recording of the process of ejection of sputtered particles from the free surface of a Pb sample, which was subjected to shock-wave loading with a maximum amplitude of the loading pressure pulse of ~ 15 GPa, in the EPC using (a, b) optical and (c) X-ray radiography methods: (1) free surface of the sample; (2) particle flow; (3) Pb standards (foil with a thickness of 30–480 μm), and (K) optical magnification factor [15].

Hence, the created research area of studies, which is based on the physically substantiated approaches to designing, experimental methods, and numerical simulation, makes it possible to develop EPCs of various purposes, which provide the industrial safety during investigations of explosive processes and during their applications in blasting technologies using explosive charges with masses in a range of a few grams to several kilograms.

REFERENCES

1. *Razrushenie raznomasshtabnykh ob"ektov pri vzryve* (Destruction of Objects of Different Scales at Explosions), Ivanov, A.G., Ed., Sarov: RFYaTs-VNIIEF, 2001.
2. Grigor'ev, D.V., Zhogin, V.P., Ivkin, A.V., Motorikin, G.P., Osipov, Yu.A., Solov'ev, V.P., Syrunin, M.A., Sysoev, N.Ya., Abakumov, A.I., Gorbenko, G.V., Nizovtsev, P.N., Fedorenko, A.G., and Tyupanov, A.A., RF Patent no. 2130563, *Byull. Izobret.*, 1997, no. 1.
3. Ivanov, A.G., Syrunin, M.A., and Fedorenko, A.G., RF Patent no. 2009387, *Byull. Izobret.*, 1994, no. 5.
4. Ivanov, A.G., Syrunin, M.A., and Fedorenko, A.G., *J. Appl. Mech. Tech. Phys.*, 2001, vol. 42, no. 1, p. 174.
5. Syrunin, M.A., Fedorenko, A.G., and Ivanov, A.G., *Combust., Explos., Shock Waves*, 2002, vol. 38, no. 3, p. 365.
6. Abakumov, A.I., Mikhailov, A.L., Syrunin, M.A., Abakumov, S.A., Devyatkin, I.V., Karpich, L.P., Mel'tsas, V.Yu., Nizovtsev, P.N., Rusak, V.N., Solov'ev, V.P., Treshchalin, S.M., Fal'chenko, A.A., Fedorenko, A.G., and Yakovlev, E.D., RF Patent no. 2244253, *Byull. Izobret.*, 2005, no. 1.
7. Vishnevetskii, E.D., Ermakov, A.B., Snopov, V.A., and Syrunin, M.A., RF Patent no. 2280234, *Byull. Izobret.*, 2006, no. 20.
8. Abakumov, A.I., Vishnevetskii, E.D., Mikhailov, A.L., Nizovtsev, P.N., Rusak, V.N., Solov'ev, V.P., Syrunin, M.A., Fedorenko, A.G., and Chernov, V.A., RF Patent no. 2257537, *Byull. Izobret.*, 2005, no. 21.
9. Syrunin, M.A., Vishnevetskii, E.D., Mikhailov, A.L., Oreshkov, O.V., Fedorenko, A.G., Tsoi, A.P., and Chernov, V.A., RF Patent no. 2367899, *Byull. Izobret.*, 2009, no. 26.
10. Syrunin, M.A., Vishnevetskii, E.D., Fedorenko, A.G., and Chernov, V.A., RF Patent no. 2404407, *Byull. Izobret.*, 2010, no. 32.
11. Syrunin, M.A., Vishnevetskii, E.D., Chernov, V.A., Abakumov, A.I., and Oreshkov, O.V., RF Patent no. 2524064, *Byull. Izobret.*, 2014, no. 21.
12. Abakumov, A.I., Devyatkin, I.V., Mel'tsas, V.Yu., Mikhailov, A.L., Portnyagina, G.F., Rusak, V.N., Solov'ev, V.P., Syrunin, M.A., Treshchalin, S.M., and Fedorenko, A.G., in *Trudy Ross. Feder. Yader. Tsentrvseross. Nauchn.-Issl. Inst. Eksp. Fiz.* (Proc. Russ. Feder. Nucl. Center-All-Russ. Sci.-Res. Inst. Exp. Phys.), Sarov: Ross. Feder. Yader. Tsentrvseross. Nauchn.-Issl. Inst. Eksp. Fiz., 2008, no. 12, p. 298.
13. Abakumov, A.I., Syrunin, M.A., Solov'ev, V.P., Mikhailov, A.L., and Mel'tsas, V.Yu., *Trudy mezhdunarodnoi konferentsii "XIII Kharitonovskie tematicheskie nauchnye chteniya"* (Proc. Int. Conf. "13th Khariton Thematic Scientific Readings"), Sarov: Ross. Feder. Yader. Tsentrvseross. Nauchn.-Issl. Inst. Eksp. Fiz., 2011, p. 441.
14. Burtsev, V.V., Lebedev, A.I., Mikhailov, A.L., Ogorodnikov, V.A., Oreshkov, O.V., Panov, K.N., Rudnev, A.V., Svirskii, O.V., Syrunin, M.A., Trutnev, Yu.A., and Khramov, I.V., *Combust., Explos., Shock Waves*, 2011, vol. 47, no. 6, p. 627.
15. Mikhailov, A.L., Ogorodnikov, V.A., Sasik, V.S., Raevskii, V.A., Lebedev, A.I., Zotov, D.E., Erunov, S.V., Syrunin, M.A., Sadunov, V.D., Nevmerzhtskii, N.V., Lobastov, S.A., Burtsev, V.V., Mishanov, A.V., Kulakov, E.V., Satarova, A.V., Georgievskaya, A.B., Knyazev, V.N., Kleshchevnikov, O.A., Antipov, M.V., Glushikhin, V.V., Yurtov, I.V., Utenkov, A.A., Sen'kovskii, E.D., Abakumov, S.A., Presnyakov, D.V., Kalashnik, I.A., Panov, K.N., Arinin, V.A., Tkachenko, B.I., Filyaev, V.N., Chapaev, A.V., Andramanov, A.V., Lebedeva, M.O., and Igonin, V.V., *J. Exp. Theor. Phys.*, 2014, vol. 118, no. 5, p. 785. DOI: doi .10.7868/S0044451014050127.
16. Ryabov, A.A., Romanov, V.I., Syrunin, M.A., Fedorenko, A.G., Tsoi, A.P., and Zefirov, S.V., *Problemy Prochn. Plast.*, 2003, no. 3, p. 122.
17. Velichko, O.M., Gubkova, G.N., Deryugin, Yu.N., Mel'tsas, V.Yu., and Portnyagina, G.F., *Sbornik dokladov nauchnoi konferentsii Volzhskogo regional'nogo tsentra RARAN "Sovremennye metody proektirovaniya i otrabotki raketno-artilleriiskogo vooruzheniya"* (Proc. Sci. Conf. Volzhsk. Region Center "Contemporary Methods of Design and Refinement of Rocket-Artillery Armament"), Sarov: Ross. Feder. Yader. Tsentrvseross. Nauchn.-Issl. Inst. Eksp. Fiz., 2000, p. 76.
18. Godunov, S.K., Zabrodin, A.V., Ivanov, M.Ya., and Prokopov, G.P., *Chislennoe reshenie mnogomernykh zadach gazovoi dinamiki* (Digital Solution of Multidimensional Problems of Gas Dynamics), Moscow: Nauka, 1976.
19. Lin, E.E., Mel'tsas, V.Yu., and Portnyagina, G.F., *Trudy Ross. Feder. Yader. Tsentrvseross. Nauchn.-Issl. Inst. Eksp. Fiz.* (Proc. Russ. Feder. Nucl. Center-All-Russ. Sci.-Res. Inst. Exp. Phys.), Sarov: Ross. Feder. Yader. Tsentrvseross. Nauchn.-Issl. Inst. Eksp. Fiz., 2003, no. 4, p. 266.
20. Abakumov, A.I., Nizovtsev, P.N., Pevnitskii, A.V., and Solov'ev, V.P., *Tezisy Dokladov mezhdunarodnoi konferentsii "IV Zababakhinskie nauchnye chteniya"* (Proc. Int. Conf. "4th Zababakhin Scientific Readings"), Snezhinsk: Ross. Feder. Yader. Tsentrvseross. Nauchn.-Issl. Inst. Eksp. Fiz., 1995, p. 89.
21. Medvedev, O.V., Egorychev, Yu.N., Mironov, D.S., Pylev, G.I., Syrunin, M.A., Shilov, O.N., Fadeev, V.Yu., and Yankov, S.A., *Mezhdunarodnaya konferentsiya "XV Kharitonovskie nauchnye chteniya"*. *Sbornik dokladov* (Proc. Int. Conf. "15th Khariton Scientific Readings"), Sarov: Ross. Feder. Yader. Tsentrvseross. Nauchn.-Issl. Inst. Eksp. Fiz., 2013, p. 785.

Translated by A. Seferov